Numerical modeling of auto-ignition of isolated fuel droplets in microgravity

Alberto Cuoci *, Alessio Frassoldati, Tiziano Faravelli, Eliseo Ranzi

Department of Chemistry, Materials, and Chemical Engineering "G. Natta", Politecnico di Milano, P.zza Leonardo da Vinci 32, 20133 Milano, Italy

Available online 10 July 2014

1. Introduction

The combustion of liquid fuels is of great interest in many practical applications, from industrial burners to diesel engines, especially because of their high-energy density per unit volume [1]. In particular, the spontaneous ignition (or auto-ignition) of fuel droplets is a very important process to be controlled effectively. However, the strong interactions between the many physico-chemical processes dominating the ignition of fuel droplets make the study of combustion of liquid fuels a very complex subject. It is thus useful to take apart the overall system and to study simpler and possibly ideal conditions. The most adopted and suitable simplification corresponds to the isolated fuel droplet system with a surrounding gas. Such a system includes all of the existing basic processes occurring in practical combustors, including heat-up, phase-change, diffusion, and chemical reactions. In addition, microgravity conditions further simplify the

* Corresponding author. Fax: +39 02 7063 8173. *E-mail address:* alberto.cuoci@polimi.it (A. Cuoci).

system, because of the spherical symmetry, which strongly reduces the required computational time and memory requirements, especially when complex kinetic schemes are adopted.

The transient behavior of droplet heating and the gas-phase mixture conditions causing the ignition are today quite well understood. Several numerical models were proposed and applied, with particular emphasis on the transient physical processes [2]. From recent works [3–5] it was recognized that a detailed description of the chemical reactions is strictly necessary to predict with reasonable accuracy not only the ignition delay times and the explosion diagrams, but also to better char-acterize the burning rates. Several efforts have been already devoted to the numerical study of auto-ignition of isolated fuel droplets with detailed chemistry, but only a few of them adopted low-tem-perature mechanisms [4,6–8]. The improving knowledge on the chemistry of hydrocarbon oxida-tion and the increasing availability of computa-tional resources now enable the possibility to simulate the auto-ignition of isolated fuel droplets with very detailed kinetic mechanisms, with hun-dreds of species.

In this paper we numerically investigate the auto-ignition of isolated fuel droplets of *n*-heptane, *n*-decane and *n*-dodecane in microgravity conditions using a detailed kinetic mechanism (460 species and more than 16,000 reactions). All the simulations are compared and validated with experimental data available in the literature. The final aim is to demonstrate the importance of the low-temperature chemistry during the auto-ignition process. To our knowledge, this is the first work in which the auto-ignition of isolated fuel droplets is numerically modeled using such a large kinetic mechanism.

2. Mathematical model

The mathematical model used to describe the transient evaporation, ignition, and combustion of isolated pure fuel droplets in microgravity conditions was presented and validated in [4]. Here, only its main features are summarized. The numerical model assumes spherical symmetry, because of the microgravity conditions. The conservation equations of energy and mass are solved both for the liquid and gas phases. In addition, the conservation equations of species are solved for the gas phase. Only the ordinary mass diffusion is taken into account in the species equations. Previous simulations including the Soret effect did not show any significant impact on the auto-ignition results [9]. The properties of the liquid are taken from Daubert and Danner's database [10]. The possible presence of internal liquid recirculations is accounted for using the simplified approach suggested in [11].

Chemical reactions in the gas phase are described using a detailed kinetic mechanism (see the next paragraph). The transport properties for species in the gas phase were either taken from the CHEMKIN transport database [12] or estimated following the procedure proposed in [13], while the thermochemical information was obtained primarily from the CHEMKIN thermodynamic database. Radiative heat fluxes were estimated by adopting the approach proposed by Kazakov et al. [14]. The Planck mean absorption coefficients were derived from polynomial expressions for CO, CO_2, and H_2O, which are assumed to be the only molecules influencing radiative transfer. Symmetry conditions are imposed at the center of the droplet. At the liquid/gas interface the continuity of fluxes of heat and species is considered. The far field boundary ($\sim$100 times the initial droplet diameter) is defined using Dirichlet's conditions (i.e. assigned ambient composition and temperature) and remains fixed in the simulations.

The resulting system includes partial differential equations and non-linear, algebraic equations (because of boundary conditions). The partial differential equations are discretized using the finite-difference method, using an adaptive grid fixed on the droplet surface. The resulting system of differential-algebraic equations is solved in a fully-coupled approach using the BzzDae solver (http://www.chem.polimi.it/homes/gbuzzi) [15].

The results reported in this work were based on a grid with 30 and 200 points for the liquid and gas phases, respectively. Simulations with a larger number of points did not show significant differences. The convective and diffusion terms were discretized using the upwind scheme and centered, 2nd order differences, respectively. The simulations were carried out on Intel® Xeon® CPU X5675 @ 3.07 GHz processors.

3. Detailed kinetic mechanism

A general, detailed kinetic scheme, called POLIMI_TOT_1311 and consisting of 460 species and more than 16,000 reactions, was used to describe combustion in the gas phase [16]. The mechanism is freely available on the web (together with thermodynamic data and transport properties) at the following address: http://creckmodeling.chem.polimi.it. The mechanism covers the low- and high-temperature regions of hydrocarbon oxidation. Further details and extensive validation can be found in [16,17] and in the Supplemental material.

4. Autoignition of isolated *n*-decane droplets

Xu et al. [18] performed several experimental measurements about vaporization and auto-ignition of isolated fuel droplets of *n*-decane in

microgravity conditions and atmospheric pressure. A quartz fiber was used to suspend the fuel droplets in the oven whose temperature was varied from 633 K to 1123 K, to test both droplet burning and vaporization.

In the following we focus the attention on the experiments at 633 K, because they give a clear evidence of the importance of low-temperature chemistry during the auto-ignition. Three different initial droplet diameters of 0.91, 1.22 and 1.57 mm were numerically studied. In these conditions, no visible flames were experimentally observed during the vaporization [18]. Figure 1 shows the experimental squared droplet diameter versus time. After the ini-tial period in which heating and liquid-phase expansion prevail on evaporation, the typical "d2-law" can be recognized. The dotted lines in Fig. 1 represent the model predictions without accounting for the reactions in the gas phase. The model completely fails in predicting the experimen-tal measurements: the calculated vaporization rates are much smaller than the measured ones. The cal-culations were then repeated using the detailed kinetic mechanism (Section 3), accounting both for low and high temperature chemistry. In this case the agreement with the experimental data is quite good and the numerical predictions are very accurate (continuous lines in Fig. 1). From the maximum temperature of the gas phase versus time (Fig. 2) we can easily recognize the formation of a low-temperature flame around the droplet. The relatively low ambient temperature prevents high-temperature ignition to occur. The temperature profiles show initial dumped cool flames and the successive attainment of a more stable temperature *plateau*. The dumping of cool flames is the combined result of the progressive consumption of fuel and gas-phase heating. Once the first cool flame ignites, the vaporized fuel is consumed and is only partially replaced by the relatively slow vaporization. The successive cool flames, characterized by

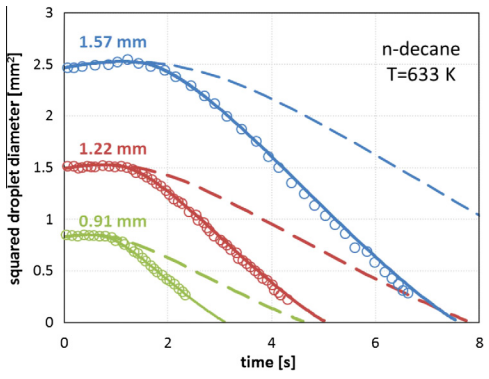

Fig. 1. Droplet squared diameters versus time of *n*-decane droplets in air. Comparison between experiments [18] and numerical results without (dotted lines) and with (continuous lines) low-temperature mechanism.

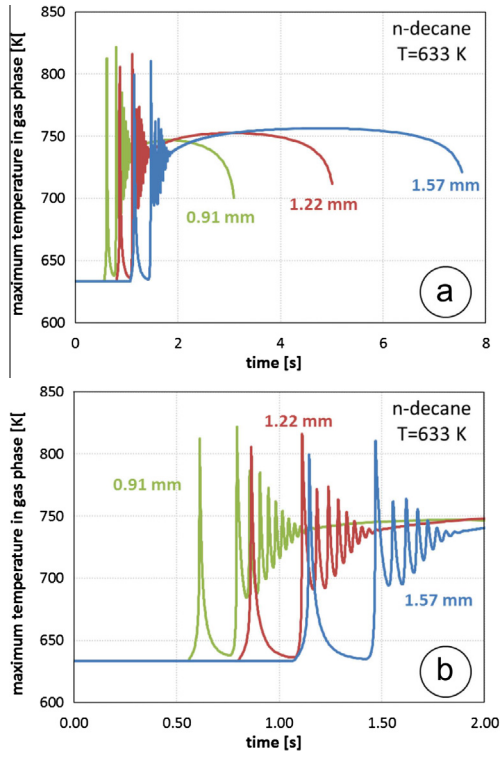

Fig. 2. Panel a: Maximum temperature in gas phase versus time for *n*-decane droplets in air at 633 K. Panel b: profile reported in panel a is zoomed to better show the features of cool flames.

higher frequencies, produce less heat, and progressively move the system from the cool flame to the slow combustion region. Under these conditions, the vaporization rates are controlled by the low-temperature mechanism. The *plateau* temperatures of the cool flames increase with increasing initial diameter, moving from ~740 K for the 0.91 mm droplet to ~760 K for the 1.57 mm droplet. This can explain the slightly higher vaporization rate for the larger droplet, which was observed both numerically and experimentally. During the dumped cool flame regime, the radial position of the peak temperature (not here reported) is very close to the droplet surface (~1.5-2.5 mm), while during the second phase (characterized by the *plateau* temperature) it slowly decreases with time.

Figure 3 shows the calculated radial profiles of temperature and main species at 3 s for the 1.22 mm droplet. The typical structure of a low-temperature flame can be recognized. Under these conditions the fuel does not fully react and the ketohydroperoxide (NC_{10}-OQOOH) is the main component, together with H_2O, H_2O_2, and CO. Fuel and oxygen can coexist also in the region close to the droplet surface and their concentration profiles are smoother than in hot-temperature

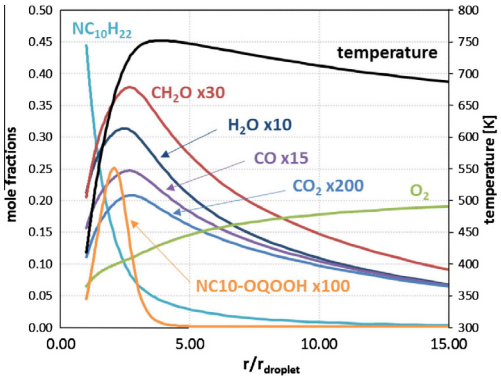

Fig. 3. Radial profiles of temperature and mole frac-tions of selected species at 3 s for *n*-decane droplet with initial diameter of 1.22 mm.

flames, because of the lower reactivity of the system. This lower reactivity means that complete combustion of the high-temperature oxidation mechanism cannot be activated, with the result that partially premixed combustion occurs.

5. Autoignition of *n*-heptane, *n*-decane and *n*-dodecane droplets: ignition delay times

Tanabe et al. [3] and Moriue et al. [19] experimentally investigated the spontaneous ignition of isolated fuel droplets of *n*-heptane, *n*-decane and *n*-dodecane in microgravity conditions. In their experiments the suspended fuel droplets (with initial diameter of 0.7–0.8 mm) were suddenly inserted into a pre-heated furnace in a pressurized chamber. Ignition delay times were measured in a wide range of operating conditions, with air at initial, uniform temperature of 500–1100 K and pressure of 1–20 bar. Ignition regions were mapped on temperature-pressure planes, as reported in Fig. 4. The types of ignition process were specified as no-ignition (NI), cool flame ignition (CF), single-stage (SI) and two-stage (2SI) ignition, similarly to what is reported in premixed gas explosion diagrams, often proposed for gaseous fuels. The ignition regions are quite similar for the three fuels: in particular, a slow reaction region at low temperatures and an explosion region with the typical hot ignition at high temperatures and pressures. The complexity of such diagrams suggests that the chemistry plays a fundamental role in controlling the auto-ignition process. In particular, the competition between the low- and high-temperature mechanisms is the main reason behind the different types of auto-ignition phenomena. In order to better explain this competition, Fig. 5 shows the maximum temperature in the gas-phase versus time for *n*-heptane droplets for selected initial ambient pressures and temperatures. At low ambient

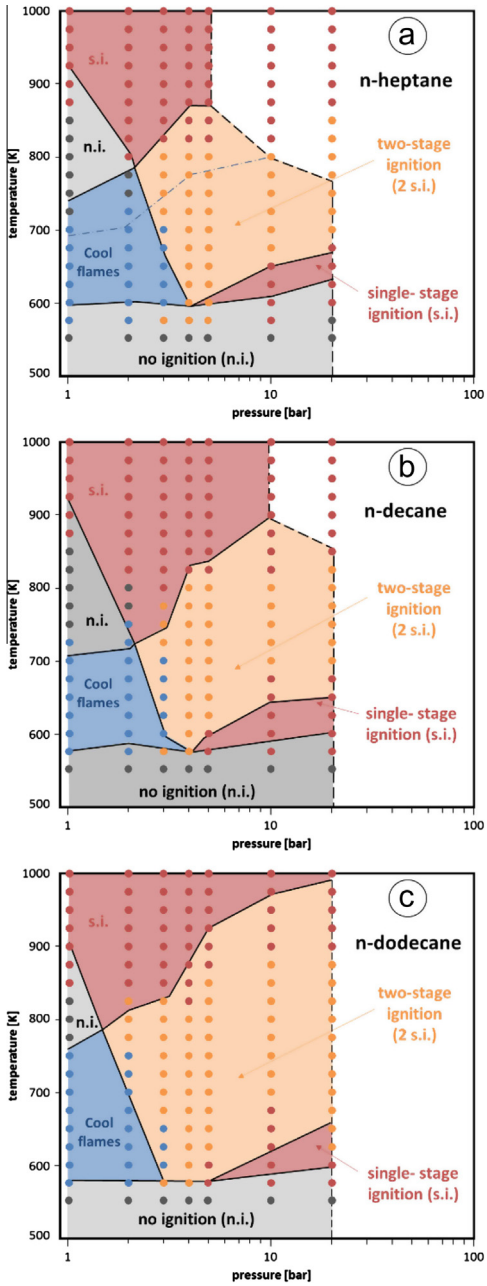

Fig. 4. Ignition regions of *n*-heptane (a), *n*-decane (b), and *n*-dodecane (c) droplets in air at different pressures and initial temperatures. Comparison between experiments (maps, d_0 = 0.7–0.8 mm) [3,19] and numerical predictions (points, $d_0 = 0.7$ mm).

temperatures, the droplet vaporizes before chemical reactions can lead to temperature increase. On the contrary, if the ambient temperature is sufficiently high for promoting the low-temperature reactions, the formation of a cool flame can be

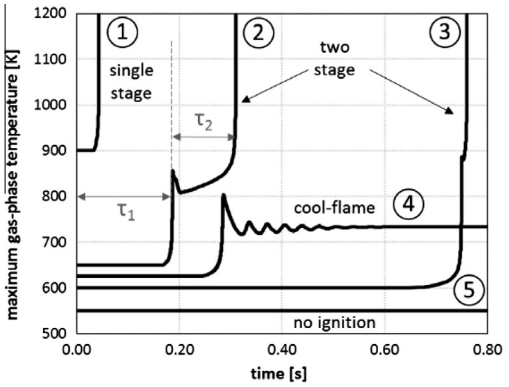

Fig. 5. Maximum gas-phase temperature versus time for *n*-heptane droplets (numerical simulations). Line 1: 5 bar, 900 K; Line 2: 5 bar, 650 K; Line 3: 1 bar, 625 K; Line 4: 5 bar, 600 K; Line 5: 1 bar, 550 K. The total induction time τ_t is the sum of the first (τ_1) and the second (τ_2) induction times.

observed, with a limited increase in the temperature. However, due to the partial oxidation of fuel by low-temperature reactions and the dilution of fuel with ambient gas because of the long time scales, the hot-ignition cannot be reached. Dumped cool flames then arises, with a successive temperature *plateau* at relatively low-temperature (see curve 4 in Fig. 5). The hot-ignition occurs only when the ambient temperature is high enough so that the high-temperature reactions becomes dominant (curve 1). Eventually, when the temperature and/or the pressure of the ambient are high enough to make the oxidation reactions competitive with heat transfer, a multi-stage ignition phenomenon can be observed, i.e. a first maximum of tempera-ture, associated to a cool flame, is followed by a *plateau* temperature and then by a hot flame igni-tion (curves 2 and 3). The first induction time is not affected only by the low-temperature chemistry, but also depends on the physics (evaporation, droplet size, etc.) and corresponds to the appearance of a cool flame. The duration of the first stage of ignition, i.e. the time from the cool flame appear-ance up to the ignition of the hot flame, is the sec-ond induction time. It depends almost entirely on the chemical kinetics.

According to what suggested by Schnaubelt et al. [6], the initial droplet temperature T_0 was set linearly from $T_0 = 300$ K at $T_a = 600$ K to $T_0 = 320$ K at $T_a = 1000$ K (where T_a is the ambi-ent temperature) in agreement with the thermo-couple measurements in the cold section of the experimental apparatus. The numerical predictions (points) were compared with the experimental data (maps and lines) in Fig. 4. The numerical calculations were able to recognize the different experimental auto-ignition behaviors, especially at low temperature.

Figure 6a shows the 2-stage ignition of a *n*-heptane droplet at 650 K and 5 bar, as a representative example. The first ignition occurs after 180 ms inserting the droplet into the combustion chamber, when the concentration of the ketohydroperoxides NC_7-OQOOH becomes sufficiently large to promote the low-temperature ignition. During the following 130 ms a cool flame burns at nearly constant temperature of 820–840 K. The radial location of the maximum cool flame temperature (not here reported) moves to the droplet surface with time and the region with high temperature (above the ambient value) gets wider. After 310 ms the hot-flame ignition occurs, as evident from the rapid increase of temperature and the sudden production of OH radicals. Fig. 6b reports the radial profiles of heat release rate (HRR) at four different times. The cool flame (curve 2) is weakly exothermic, if compared to the HRR during the ignition (curve 3). The nega-tive values of the HRR in proximity of the droplet

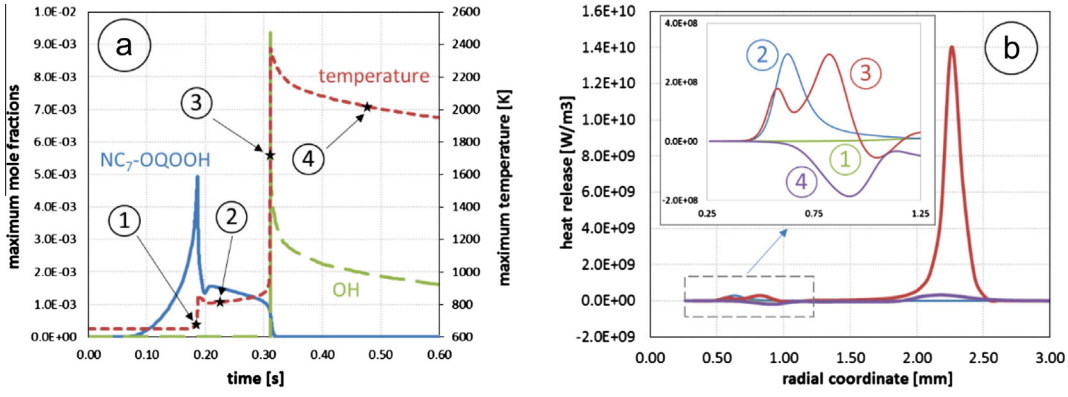

Fig. 6. Auto-ignition of *n*-heptane droplet at 650 K and 5 bar. Panel a: Maximum values of mole fractions of NC7-OQOOH and OH and temperature versus time. Panel b: Radial profiles of heat release at the four different times, reported on the left panel.

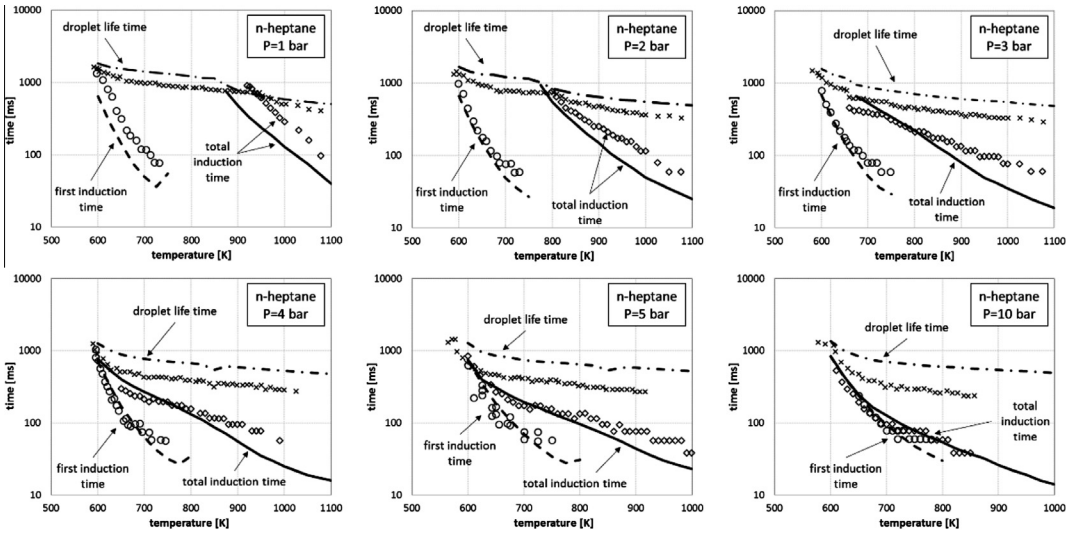

Fig. 7. Comparison between experiments (points) and simulations (lines) for auto-ignition of *n*-heptane droplets: first (○ and dashed lines) and total (◇ and continuous lines) induction times, and droplet life time (× and dashed-dotted lines).

surface for the hot-flame (curve 4) is due to the endothermic reactions of fuel pyrolysis.

Figure 7 shows the satisfactory comparisons between the predicted and the experimental [3] first and total ignition times for *n*-heptane droplets. As already observed by Schnaubelt et al. [6], who did numerical simulations at the pressure of 5 bar, the numerical model under-estimates the ignition delay time at high temperatures. The first and total induction times tend to decrease with increasing the ambient temperature, since the vaporization of the fuel droplet is enhanced. At pressures of 4 and 5 bar the Zero Temperature Coefficient (ZTC) region is evident in the range of tempera-tures between 700 K and 750 K. In this region the second induction time, which is the time to activate the high-temperature reactions, does not depend on changes in ambient temperature. The Negative Temperature Coefficient (NTC) region, typically observed in homogeneous gas-phase mix-tures, is not seen because of the inhomogeneous fields of temperature and composition around the vaporizing droplet. The total induction time decreases with increasing the pressure, because of the higher reactivity of the system. On the contrary, since the ambient pressure reduces the vaporization rate, the first induction time, significantly influenced by the physical processes, increases with increasing the pressure. Figure 7 shows also the comparison between the measured [3] and calculated droplet life-times. The numerical life-time was defined as the time at which the droplet volume is 1/1000 of the initial volume, but from Tanabe et al. [3] it is not clear the precise definition of the experimental life-time. Therefore it is not possible to explain why the numerical simulations always over-estimate the measured life-times.

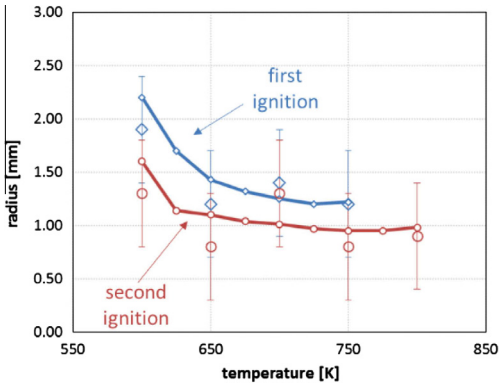

Fig. 8. Ignition radii for *n*-heptane droplets at $P = 5$ bar. Comparison between experiments (points with error bars) [20] and numerical results (lines).

Figure 8 shows the a comparison of cool and hot flame ignition radii between experiments [20] and numerical simulations for the *n*-heptane droplets at 5 bar, at ambient temperatures between 600 K and 800 K. Predicted and measured ignition radii are of the same order and within the experimental error. The simulations show that the ignition radius for the cool flame has a minimum around ~700 K. At ambient temperatures higher than ~650 K the hot ignition radius is ~20–25% smaller than the cool flame ignition radius.

6. Conclusions

The auto-ignition of isolated fuel droplets of *n*-heptane, *n*-decane and *n*-dodecane was numerically investigated using a detailed kinetic mechanism in a wide range of operating conditions,

with ambient temperatures and pressures covering the 600–1000 K and 1–20 bar ranges, respectively. The model was able to correctly identify the typical auto-ignition regimes of *n*-alkane oxidation. Both first-stage and total induction times were reasonably captured by the numerical simulations. The low-temperature chemistry was found to play a fundamental role when the ambient temperature was not sufficiently high for promoting directly the hot-temperature combustion reactions.

Characterization of the gas-phase environment in terms of pollutants like NOx, aldehydes, PAHs (Polycyclic Aromatic Hydrocarbons) and soot can be easily managed through proper detailed kinetic schemes. Eventually, the application to real and complex fuels, such as diesel or jet fuels, makes this numerical model a powerful tool for deeper and more complete investigations about spray ignition.

Acknowledgements

The authors acknowledge Alessandro Stagni (Politecnico di Milano) for providing the validation of the kinetic mechanism. The Italian MSE and CNR-DIITET are acknowledged for their financial support (Project Number D44G120000 40001).

Appendix A. Supplementary data

Supplementary data associated with this article can be found, in the online version.

References

[1] V. Nayagam, J.B. Haggard Jr., R.O. Colantonio, A.J. Marchese, F.L. Dryer, B.L. Zhang, F.A. Williams, *AIAA J.* 36 (8) (1998) 1369–1378.

[2] S.S. Sazhin, *Prog. Energy Combust. Sci.* 32 (2) (2006) 162–214.

[3] M. Tanabe, C. Bolik, C. Eigenbrod, H.J. Rath, J. Sato, M. Kono, Twenty-Sixth Symposium (International) on Combustion/The Combustion Institute, (1637–1642) (1996).

[4] A. Cuoci, M. Mehl, G. Buzzi-Ferraris, T. Faravelli, D. Manca, E. Ranzi, *Combust. Flame* 143 (3) (2005) 211–226.

[5] T.I. Farouk, F.L. Dryer, *Combust. Flame* 161 (2) (2014) 565–581.

[6] S. Schnaubelt, O. Moriue, T. Coordes, C. Eigenbrod, H.J. Rath, *Proc. Combust. Inst.* 28 (2000) 953–960.

[7] S. Schnaubelt, O. Moriue, C. Eigenbrod, H.J. Rath, *Microgravity Sci. Technol.* XIII (1) (2001) 20–23.

[8] S. Schnaubelt, C. Eigenbrod, H.J. Rath, *Microgravity Sci. Technol.* XVII (3) (2005) 5–9.

[9] A. Cuoci, A. Frassoldati, T. Faravelli, F.A. Williams, 29th American Society for Gravitational and Space Research & 5th International Symposium for Physical Sciences in Space, Orlando (USA), (2013).

[10] T.E. Daubert, R.P. Danner, *Data Compilation Tables of Properties of Pure Compounds*, Design Institute for Physical Property Data, American Institute of Chemical Engineers, 1985.

[11] A.J. Marchese, F.L. Dryer, *Combust. Flame* 105 (1–2) (1996) 104–122.

[12] R.J. Kee, F. Rupley, J.A. Miller, Sandia Report SAND89-8009 - Sandia National Laboratories, (1989).

[13] H. Wang, M. Frenklach, *Combust. Flame* 96 (1994) 163–170.

[14] A. Kazakov, J. Conley, F.L. Dryer, *Combust. Flame* 134 (4) (2003) 301–314.

[15] G. Buzzi-Ferraris, D. Manca, *Comput. Chem. Eng.* 22 (11) (1998) 1595–1621.

[16] E. Ranzi, A. Frassoldati, R. Grana, A. Cuoci, T. Faravelli, A.P. Kelley, C.K. Law, *Prog. Energy Combust. Sci.* 38 (4) (2012) 468–501.

[17] A. Stagni, A. Cuoci, A. Frassoldati, T. Faravelli, E. Ranzi, Industrial & Engineering Chemistry Research, in press (doi: http://dx.doi.org/10.1021/ie403272f), (2014).

[18] G. Xu et al., *Int. J. Heat Mass Transfer* 46 (2003) 1155–1169.

[19] O. Moriue, C. Eigenbrod, H.J. Rath, J. Sato, K. Okai, M. Tsue, M. Kono, *Proc. Combust. Inst.* 28 (2000) 969–975.

[20] S. Schnaubelt, M. Tanabe, C. Eigenbrod, H.J. Rath, *Proc. Drop Tower Days* (1998) 299–306.